Duzce University Journal of Science and Technology
Düzce Üniversitesi Bilim ve Teknoloji Dergisi
14 (1), 2026, 60-71.
https://doi.org/10.29130/dubited.1739006
e-ISSN: 2148-2446
https://dergipark.org.tr/en/pub/dubited



Research Article

Prediction of Sector and Region for Three-Level NPC Inverters Using Artificial Neural Networks

Fatih Özen[1*], Rana Ortaç Kabaoğlu[2], Tarık Veli Mumcu[2]

[1] Tekirdağ Namık Kemal University, Vocational College of Technical Sciences, Department of Electronics and Automation, Tekirdağ, Türkiye. ror.org/01a0mk874

[2] İstanbul University-Cerrahpaşa, Faculty of Engineering, Department of Electrical- Electronics Engineering, İstanbul, Türkiye. ror.org/01dzn5f42

*Corresponding author:
fozen@nku.edu.tr

Received: 09.07.2025
Revision: 07.09.2025
Accepted: 16.10.2025
Available Online: 21.01.2026

Abstract: The performance of inverters, the most important hardware unit of renewable energy systems, depends on the sector and region values in which they operate in relation to the reference voltage vector. The accurate identification of sectors and regions is crucial. This study aims to overcome the shortcomings of sector and region identification based on classical mathematical models. To this end, the identification of sectors (6 classes) and regions (4 classes) is predicted with highly accuracy using artificial neural network (ANN) architectures. In this context, Narrow, Medium, Wide, Bilayered and Trilayered architectures were used and systematically compared. For sector detection, Narrow NN and Wide NN showed the highest performance with 99.97% accuracy. For region detection, Wide NN has the highest performance among the other architectures with 98.81% accuracy. The proposed architecture is modelled in a simulation environment and analyzed in terms of inverter sector and region, output current and voltage values. The simulation results show that the models based on classical and artificial neural networks are compatible and provide a solution to reduce the processing load.

Keywords: *Inverter, sector and region, artificial neural networks*

I. INTRODUCTION

Inverters are key components for renewable energy systems and industrial applications with high power requirements (Kadhim & Hasan, 2024). They play a crucial role in energy conversion processes by converting direct current into alternating current (Sirohi et al., 2024). Thanks to its ability to generate output signals with the desired amplitude and frequency, it has a wide range of applications in both single-phase and three-phase systems (Annoukoubi et al., 2024). Nowadays, renewable energy sources have gained importance due to limited reserves and the environmental impact of fossil resources, and accordingly the role of inverters in energy systems has become even more important (Hassan et al., 2024; Khalid, 2024). Multilevel inverter structures, which were developed to reduce switching losses in semiconductor elements for high-performance applications, are characterized by high efficiency and low harmonic distortion (Munawar et al., 2024; Chouhan et al., 2024).

The efficiency of these systems depends on precise control of the inverter's output voltage levels and accurate identification of sectors and regions based on the reference voltage vector (Cavdar & Ozcira Ozkilic, 2024). Sector and region information are the basic parameters for determining switching strategies in multilevel inverters. If they are not determined correctly, undesirable situations such as overloading of the power electronic elements, increased losses, voltage imbalances and overall distortions will occur (Shiny & Baiju, 2009; Yan et al., 2022). It is therefore of great importance to develop methods for identifying sectors and regions in order to ensure high performance and stable operation of inverter systems (Wang et al., 2025).

The classic method for sector and region detection in inverters is based on fixed equations, trigonometric calculations, and predefined rules (Ramadan et al., 2024). However, threshold-based approaches cannot achieve the desired results for reasons such as sudden load changes, temperature effects due to electronic components and voltage fluctuations (Sarhan et al., 2024). The methods of artificial neural networks, which are able to learn non-linear and multidimensional system behavior, are a good alternative for the recognition of sectors and regions. Neural networks quickly find solutions to complex patterns with training data without the need for fixed equations and are more flexible and adaptable to unexpected system variations (Ghadi et al., 2023). Classic algorithms lead to delays in real-time control systems as they increase the processor load. Artificial neural networks, on the other hand, facilitate integration into real-time applications by providing faster predictions after training (Arslan, 2024).

In the literature, artificial neural networks have been found to be used in inverter systems, especially in areas such as sector and region recognition, fault detection, and control strategy classification. Yan Y et al. (Yan et al., 2024) In their

Cite as: Özen, F., Ortaç Kabaoğlu, R., & Mumcu, T. V. (2026). Prediction of sector and region for three-level NPC inverters using artificial neural networks. *Duzce University Journal of Science and Technology, 14*(1), 60-71. https://doi.org/10.29130/dubited.1739006

This is an open access paper distributed under the terms and conditions of the Creative Commons Attribution-NonCommercial 4.0 International License.

study, they used artificial neural network methods to eliminate model complexity in three-level NPC inverters and perform fault detection by monitoring the current value at the output. Visma A et al. (Viswa Teja et al., 2023) In their study, they used a maximum power point tracking (MPPT) controller based on an artificial neural network (ANN) to regulate the signal of photovoltaic batteries and increase their output. Bakeer A et al. (Bakeer et al., 2022) In their study, they presented a control strategy based on artificial neural networks that does not require a predefined mathematical model of the inverter. In this study, they determined the optimal switching states of the inverter.

In this study, a three-level inverter of the Neutral Point Clamped (NPC) type is modelled and analyzed. The inverter model involves the application of the output signals obtained by varying parameters such as input voltage, switching frequency and modulation index to an R-L load. In this modelling process, artificial neural network techniques were used to reduce the computational load of the system and improve computational efficiency. In this way, sector and region predictions based on the input parameters of the system can be realized with high accuracy.

The motivation and contributions of this study are that it is an innovative and efficient model based on a lightweight, low-depth and high-precision artificial neural network architecture developed for sector and region detection in three-level NPC inverters; the proposed wide neural network-based model provides computational efficiency, high classification performance and an optimized solution compared to many heavy-structured ANN models in the literature; and easy integration into hardware-based systems.

The rest of this paper is organized as follows: In Section II, the general principle of operation of a three-level inverter, the preparation of the dataset, neural network techniques and performance evaluation metrics are explained in detail. In Section III, comprehensive results and findings are presented. Finally, the conclusions and potential of the study are discussed in Section IV.

II. MATERIAL AND METHOD

The steps of the model developed in this study to recognize sectors and regions for inverters are shown in Figure 1. The proposed approach mainly consists of four steps: three-level diode-clamped (NPC) inverter, data set acquisition from the NPC inverter, preprocessing to check missing data and parameter normalization, and finally the use of neural network techniques for sector and zone detection. The detailed description of the individual steps is as follows.

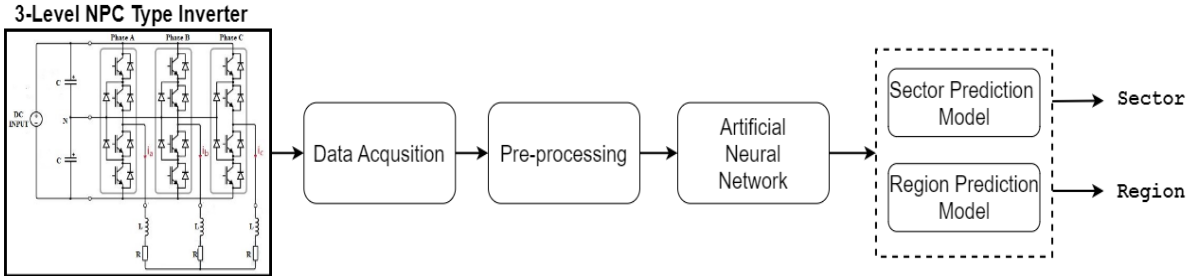

Figure 1. Framework of artificial neural network -based approach for sector and region detection models.

A. *3-Level NPC Inverter*

The three-level diode-clamped inverter (NPC) is one of the topologies used to convert direct current (DC) into alternating current (AC) with the desired amplitude and frequency (Kapustin & Shchurov, 2023). This type of inverter outperforms conventional two-level inverter structures with the advantages of lower total harmonic distortion (THD), higher energy efficiency and an improved output voltage waveform (Sathik, 2023). The structure of the NPC inverter consists of semiconductor switching elements, diodes and capacitors that can supply different voltage levels (Jayakumar et al., 2021).

Figure 2 shows a three-phase three-level diode-clamped inverter circuit of the NPC type, which feeds an R-L load. To determine the level of the inverter output voltage, four IGBTs are switched accordingly in each phase. Depending on the state of the switching elements, three different voltage levels are generated at the output of the inverter, namely $+\frac{V_{DC}}{2}$, 0 and $-\frac{V_{DC}}{2}$ (Qashqai et al., 2023).

Capacitors at the input divide the input DC voltage level into two equal levels so that the output voltage is symmetrical. There are two diodes in each phase which serve to maintain the voltage balance of the neutral point. They help to generate the correct positive and negative voltage levels.

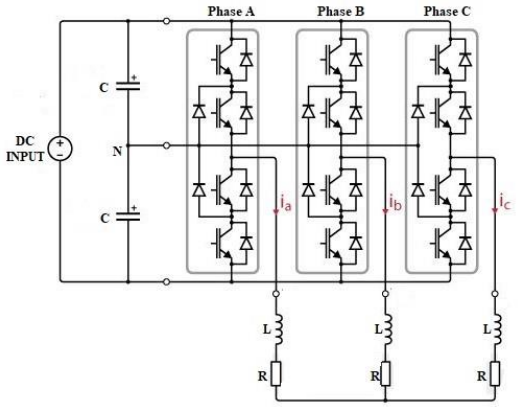

Figure 2. Three-phase 3-level inverter with diode terminals for supplying an R-L load.

B. Data Acquisition and Preparation

In inverters, the three-phase voltage or current is converted to a two-phase axis using the Clarke transform to recognize sectors and regions. One of the main objectives of this study is to obtain data from a three-phase NPC type inverter using the space vector pulse width modulation technique for sector and region detection. In a three-phase system, the phase voltages are expressed as V_a, V_b, V_c. The three phases are transformed into a two-axis (α, β) coordinate system using the Clarke transformation:

$$\begin{bmatrix} V_d \\ V_q \end{bmatrix} = \begin{bmatrix} 1 & -\frac{1}{2} & -\frac{1}{2} \\ 0 & \frac{\sqrt{3}}{2} & -\frac{\sqrt{3}}{2} \end{bmatrix} \begin{bmatrix} V_a \\ V_b \\ V_c \end{bmatrix} \quad (1)$$

After the Clark transformation, the reference voltage vector (V_{ref}) and the angle (α) are determined for the detection of sectors and regions. These values are expressed as follows:

$$V_{ref} = \left(\sqrt{{V_d}^2 + {V_q}^2}\right) \quad (2)$$

$$\alpha = \left(tan^{-1}\frac{V_q}{V_d}\right) \quad (3)$$

Figure 3 shows the space vector diagram of a three-level inverter (Hossain et al., 2024). The space vector has a hexagonal structure with six sectors (A-F). Each sector has four (1-4) triangular regions.

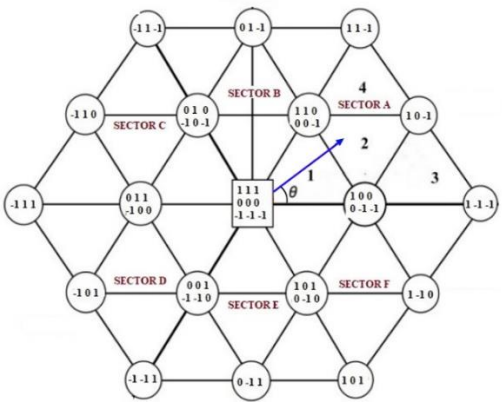

Figure 3. Space vector diagram of the three-level inverter.

Since the number of levels in the inverter is n=3, there are 3^3 switching states totaling 27. There are 24 active voltage vectors, 6 voltage vectors are large with a value of $\frac{2*V_{DC}}{3}$, 6 voltage vectors are medium with a value of $\frac{V_{DC}}{\sqrt{3}}$ and 12 voltage vectors are small with a value of $\frac{V_{DC}}{3}$ (Pal et al., 2022). This ensures that the output signal is closer to a sinusoidal shape.

The sector in which the reference voltage vector is located can be determined using the space vector diagram. The relationship between sector and angle (α) is shown in Table 1.

Table 1. Angle and sector relationship for inverter.

Sector	Angle (α)
A	$0^\circ \leq \alpha \leq 60^\circ$
B	$60^\circ \leq \alpha \leq 120^\circ$
C	$120^\circ \leq \alpha \leq 180^\circ$
D	$180^\circ \leq \alpha \leq 240^\circ$
E	$240^\circ \leq \alpha \leq 300^\circ$
F	$300^\circ \leq \alpha \leq 360^\circ$

In the inverter model used in this study, there are triangular regions within each sector. In inverters with $n = 3$ levels, there are (n-1).2, i.e., four regions. The components $m_1 and\ m_2$ of V_{ref}, which is the reference voltage vector, are found and the region is determined by using Table 2.

Table 2. Relationship between reference voltage and region for inverters.

m_1	m_2	$m_1 + m_2$	Region
<1/2	*<1/2*	*<1/2*	1
<1/2	*<1/2*	*> 1/2*	2
-	*> 1/2*	-	3
> 1/2	-	-	4

In a three-level NPC inverter, the space vector pulse width modulation (SVPWM) method is used to determine the switching sequences of the power electronic elements (Xue et al., 2020). The switching sequences and times of the power electronic elements are optimized according to the position of the reference voltage vector in the space vector diagram (Laib et al., 2020). The times are given as T_a , T_b and T_c according to the position of the reference vector in the region within the sector. The sum of the switching times, T_s, is the sum of the execution time of each vector (Kocalmış Bilhan & Emikönel, 2022). Table 3 shows the switching times and switching sequences for sector A (Subbulakshmy & Palanisamy, 2023). The variable k is expressed in Equation 5.

$$T_S = T_a + T_b + T_c \tag{4}$$

$$k = \sqrt{3} \cdot V_{ref} \cdot V_{DC}.T_S \tag{5}$$

Table 3. Switching time and sequences by region for sector A.

	Switching time	Switching sequences
Region-1	$T_a = 2.k.\sin(\ (\pi/3) - \alpha)$	(-1, 0, 0, 1, 1, 1)
	$T_b = T_s - (2.k.\sin((\pi/3) + \alpha))$	(-1, -1, 0, 0, 0,1, 1)
	$T_c = 2.k.\sin(\alpha)$	(-1, -1, -1, 0, 0, 0, 1)
Region-2	$T_a = T_s - (2.k.\sin(\alpha))$	(0, 1, 1, 1)
	$T_b = 2.k.\sin((\pi/3) + \alpha)) - T_s$	(-1, -1, 0, 0)
	$T_c = T_s - (2.k.\sin((\pi/3) - \alpha))$	(-1, -1, -1, 0)
Region-3	$T_a = (2.k.\sin(\alpha)) - T_s$	(0, 1, 1, 1, 1)
	$T_b = 2.k.\sin((\pi/3) - \alpha))$	(-1, 1, 0, 0, 1)
	$T_c = 2.T_s - (2.k.\sin((\pi/3) + \alpha))$	(-1, -1, -1, 0, 0)
Region-4	$T_a = 2.T_s - (2.k.\sin((\pi/3) + \alpha))$	(0, 1, 1, 1)
	$T_b = 2.k.\sin(\alpha)$	(0, 0, 1, 1)
	$T_c = 2.k.\sin((\pi/3) - \alpha)) - T_s$	(-1, -1, -1, 0)

C. Pre-processing

There are criteria that influence the accuracy of the model created with artificial neural networks. The most important of these criteria are data quality control, subsampling and normalization (Song et al., 2021). The data quality control phase consists of extracting data that is damaged, missing or contains physically meaningless values. The data control phase is followed by the subsampling phase, in which the data density is reduced, and the processing time is optimized without loss of information (Dhiman et al., 2023). In artificial neural network models, the scales of the independent variables can vary. Differences in scale can lead to misinterpretations of model parameters and to an unbalanced functioning of optimization processes. To avoid this problem, normalization or standardization is carried out (Cooper, 2022).

D. Artificial Neural Network

Artificial Neural Networks (ANNs) are multilayered and parameterized computational models designed to emulate the information processing capabilities of the human brain A typical ANN is composed of an input layer, one or more hidden layers, and an output layer. Each layer receives information from the previous layer through weighted connections and applies a non-linear activation function to generate its output (Ghadi et al.,2023; Atar et al.,2023). The output of a single neuron can be expressed as:

$$y = f\left(\sum_{i=1}^{n} w_i\, x_i + b\right) \tag{6}$$

where x_i represents the input features, w_i the trainable weights, b the bias term, and $f(\cdot)$ the activation function, which can be ReLU, sigmoid, or tanh.

During the training process of ANNs, the error between the predicted output $\hat{y}$ and the actual target y value is calculated, and the weighting values of the network are updated. The aim is therefore to learn parameter combinations that minimize this error (Krithiga & Mohan, 2022). Thanks to their ability to model non-linear and complex relationships, ANNs offer effective solutions for applications that require high accuracy, such as sector and region recognition, especially in models for multilevel inverters. The right choice of architecture and training strategy has a direct impact on the performance of the model. In this study, the Narrow, Medium, Wide, Bilayered and Trilayered neural network (NN) architectures are used for the prediction of sectors and regions.

The architecture of a Narrow NN with a single hidden layer and a limited number of neurons offers lower computational costs (Horiuchi et al., 2020). Narrow NN is defined as follows:

$$y = f^{(2)}\left(W_2 f^{(1)}(W_1 x + b_1) + b_2\right) \tag{7}$$

where x is the input vector, W_1 and b_1 denote the weights and biases of the hidden layer, and W_2 and b_2 are the parameters of the output layer. Narrow NNs offer low computational complexity but have limited representational capacity.

The learning ability of the Medium NN structure with a medium hidden layer is improved by increasing the number of neurons (Yarikkaya & Vardar, 2023). The structure of the model is like that of the previous model and is expressed by Eq. (7). Increasing the number of neurons enhances the learning ability and prediction accuracy while maintaining relatively low computational cost. A Wide NN is an architecture with a large number of neurons in a single layer and a large learning capacity (Zhang et al., 2021). The significantly larger hidden dimension mmm increases the model's capacity to approximate complex functions. However, this comes with higher computational requirements and a greater risk of overfitting.

The Bilayered NN extends the architecture to two hidden layers, enabling the network to capture more complex non-linear relationships (Zhang et al., 2022). The Bilayered NN is expressed as follows:

$$y = f^{(3)}\left(W_3 f^{(2)}\left(W_2 f^{(1)}(W_1 x + b_1\right) + b_2\right) + b_3) \tag{8}$$

where W_1, W_2 and b_1, b_2 correspond to the first and second hidden layers, $f^{(1)}$, $f^{(2)}$ are the respective activation functions, and W_3, b_3 define the output layer. This deeper structure allows hierarchical feature extraction, improving non-linear approximation.

A Trilayered NN architecture consists of three hidden layers. It is suitable for multi-dimensional and complex data. This model increases the number of parameters and the training time, but the accuracy performance generally improves (Alharbi & Altarjami, 2024; Khan et al., 2022). The Trilayered NN can be defined as:

$$y = f^{(4)}\left(W_4 f^{(3)}\left(W_3 f^{(2)}(W_2 f^{(1)}(W_1 x + b_1) + b_2\right) + b_3) + b_4\right) \quad (9)$$

The neural network architectures described above offer distinct advantages depending on their depth and configuration. Each model was systematically optimized through hyperparameter tuning to maximize predictive performance for the sector and region prediction tasks. In this study, the input variables to the networks were the DC input voltage (V_{dc}), modulation index (m), switching frequency (f_s), and angle (α), while the output variables were the sector and region.

The number of layers, neurons per layer, and activation functions were determined using a grid-search algorithm. The number of layers varied from 1 to 3, and the number of neurons in each layer varied from 10 to 100 in increments of 10. Based on the grid-search results, a single-layer configuration was adopted for the Narrow, Medium, and Wide NNs, with 10, 25, and 100 neurons in the hidden layer, respectively. For the Bilayered NN, a two-layer architecture with 10 neurons per layer was chosen, whereas the Trilayered NN employed a three-layer configuration, also with 10 neurons per layer. In all models, the ReLU activation function was used to introduce non-linearity.

E. Performance metrics

In this study, artificial neural network models are used to recognize sectors and regions in 3-level NPC inverters. For multi-class classification, accuracy, precision, recall, F1-score, and Matthews correlation coefficient (MCC) performance metrics are mathematically defined as follows, where k represents the true class:

$$Accuracy = \frac{\sum_{i=1}^{n} C_{i,i}}{\sum_{i=1}^{n}\sum_{j=1}^{n} C_{i,j}} \quad (10)$$

$$Precision_k = \frac{C_{k,k}}{\sum_{i=1}^{n} C_{i,k}} \quad (11)$$

$$Recall_k = \frac{C_{k,k}}{\sum_{j=1}^{n} C_{k,j}} \quad (12)$$

$$F1_k = \frac{2 \cdot Precision_k \cdot Recall_k}{Precision_k + Recall_k} \quad (13)$$

$$MCC = \frac{N \cdot \sum_i C_{i,i} - \sum_i T_i \cdot P_i}{\sqrt{\left(N^2 - \sum_i T_i^2\right)\left(N^2 - \sum_i P_i^2\right)}} \quad (14)$$

T_i and P_i represent the number of samples of the actual class i and the number of predicted samples respectively. N stands for the total number of samples. The confusion matrix is used to calculate the performance metrics, and the confusion matrix C for n classes is given by:

$$\boldsymbol{C} = \begin{bmatrix} C_{1,1} & C_{1,2} & \cdots & C_{1,n} \\ C_{2,1} & C_{2,2} & \cdots & C_{2,n} \\ \vdots & \vdots & \ddots & \vdots \\ C_{n,1} & C_{n,1} & \cdots & C_{n,n} \end{bmatrix} \quad (15)$$

F. Experimental Setup

In this study, Narrow, Medium, Wide, Bilayered and Trilayered NN architectures are used for the estimation of sectors and regions in a three-level NPC type inverter. The input DC voltage (V_{dc}), modulation index (m), switching frequency (f_s) and angle (α) are used as inputs. Figure 4 shows the data set used to create an NPC inverter model in the Matlab Simulink environment (Matlab R2021b, Mathworks, Inc., Matick, MA, USA). A dataset of approximately 360,000 rows of data was used to develop classification models for predicting sectors and regions. By using 1:12 subsampling of the data, the data density was reduced and the processing time optimized. Once the normalization process was applied to the final data set, more stable model learning was achieved. The performance of the models was evaluated using accuracy, precision, recall, F1-score and MCC metrics.

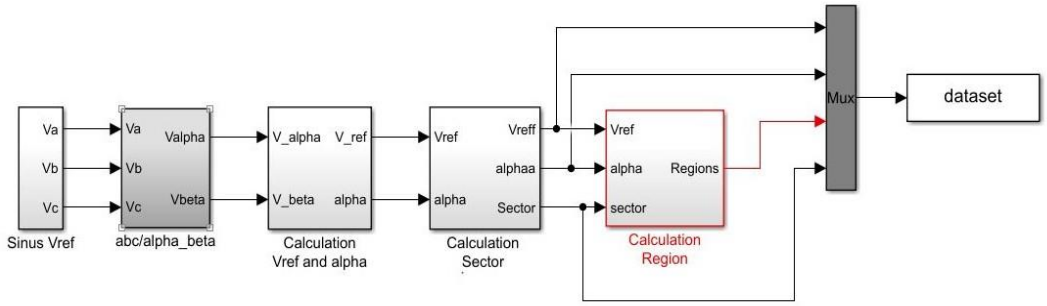

Figure 4. General concept of modeling and data acquisition.

III. RESULTS AND DISCUSSIONS

In this section, the simulation results of the developed three-level NPC inverter model are evaluated using conventional and artificial neural network methods.

A. Simulation results of traditional approach

The modelling of a 3-level inverter of type NPC was carried out in the Matlab Simulink environment. The parameters selected for the inverter model and their values are listed in Table 4.

Table 4. Parameters and values for the NPC type inverter.

Parameters	Value
DC Input Voltage	400 V
Switching frequency	5kHz
Modulation Index	0,85
Load Resistance	20 Ω
Inductance	30 mH

In this study, the results of the simulation model are analyzed using the parameters listed in Table 4. As a result of the simulation, the phase voltage (Va), the line-to-line voltage (Vab), the phase currents (Ia, Ib, Ic), the sector and region curve of the space vector at the output of the inverter were determined. The simulation results are shown in detail in Figure 5 and 6.

The phase voltage, the line-to-line voltage and the phase currents at the output of the inverter are shown in Figure 5. The results show that the phase voltage fluctuates between -198 V and +198 V (Figure 5a). The simulation results of the line-to-line voltage (Vab) show that it fluctuates between 398 V and -398 V (Figure 5b). The phase currents at the output of the inverter are also shown in Figure 5c. The phase currents (Ia, Ib, Ic) have a peak-to-peak amplitude (p-p) of 17.102 A and show a phase difference of 120° to each other. Figure 6 shows the results of the space vector diagram at the inverter output. In the space vector analysis, it can be seen that the sector values vary between 1 and 6, while the values of the regions are between 2 and 4.

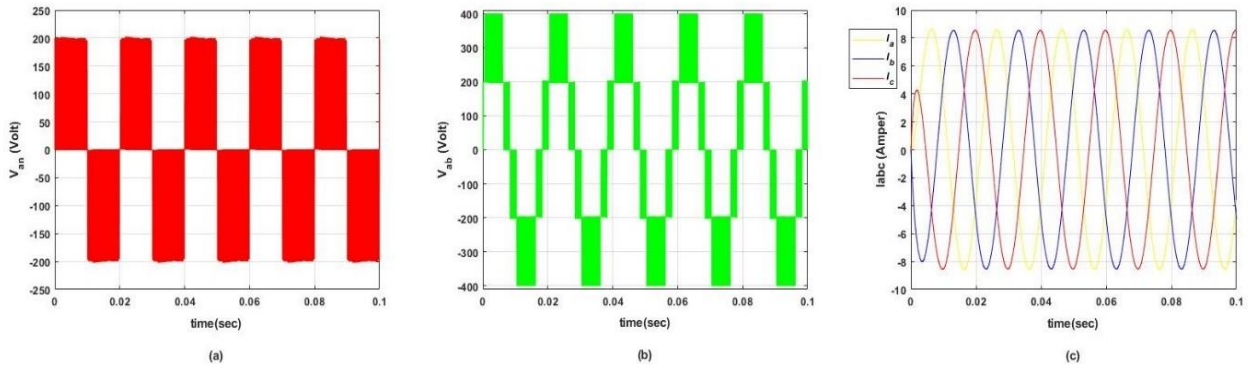

Figure 5. Inverter output simulation results (a) phase voltage (Va), (b) line-to-line voltage (Vab), (c) phase currents (Ia, Ib, Ic).

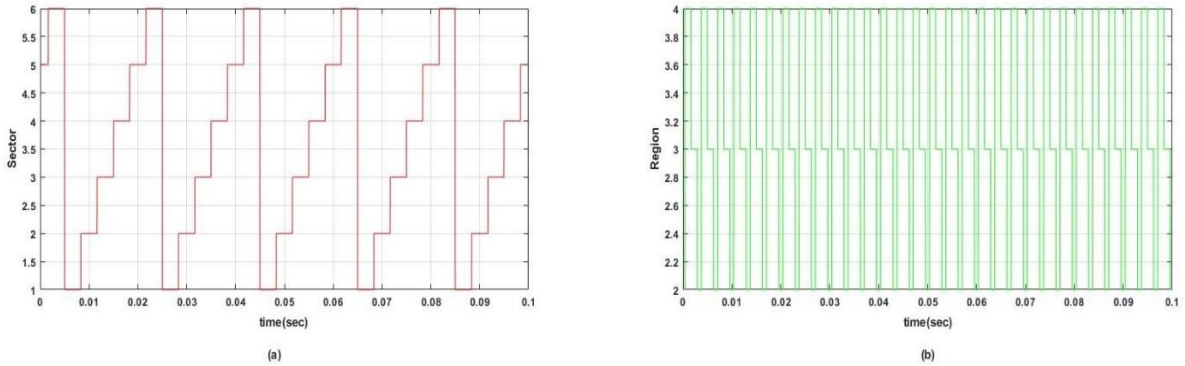

Figure 6. Inverter output space vector diagram simulation results (a) sector, (b) region.

B. Simulation results of artificial neural network models

This section evaluates the results obtained by using Narrow-NN, Medium-NN, Wide-NN, Bilayered-NN and Trilayered-NN architectures to solve the problem of predicting sectors and regions. The performance of the prediction models is analyzed using metrics such as accuracy, precision, recall, F1-score and MCC in the experiments performed using the 5-fold cross-validation method.

The classification results obtained by 5-fold cross-validation for the prediction of sectors and regions are shown in Table 5 and Table 6. The performance evaluation of the NN models was performed comprehensively by considering the average of all convolutions.

Table 5. Sector prediction results obtained using neural network models.

Models	Acc (%)	Pre (%)	Rec (%)	F1 (%)	MCC
Narrow	99.97	99.97	99.97	99.97	1.000
Medium	99.95	99.95	99.95	99.95	0.999
Wide	99.97	99.97	99.97	99.97	1.000
Bilayered	99.96	99.96	99.96	99.96	0.999
Trilayered	99.86	99.86	99.86	99.86	0.998

Table 6. Region prediction results obtained using neural network models.

Models	Acc (%)	Pre (%)	Rec (%)	F1 (%)	MCC
Narrow	50.57	47.14	53.96	46.11	0.243
Medium	63.65	60.82	65.56	61.32	0.441
Wide	98.81	98.65	98.83	98.74	0.981
Bilayered	62.37	59.18	63.63	59.34	0.417
Trilayered	72.41	70.28	78.13	71.80	0.594

The results of the sectoral prediction in Table 5 show that all models have a high performance. The models Narrow NN and Wide NN showed the best performance. The average accuracy value of both models was calculated to be 99.97 %. These two models also have the highest value for the MCC metric with a value of 1.

The performance metric results of the neural network models used for region prediction are shown in Table 6. The results show that the wide neural network model has the highest performance in terms of all performance metrics. For region predictions, the wide NN model has an accuracy of 98.81%, a precision of 98.65%, a recall of 98.83%, an F1 score of 98.74% and a Matthews correlation coefficient of 0.981.

The confusion matrix of the Wide-NN model, which shows the best performance in predicting sectors and regions, is shown in Figure 7. As can be seen in Figure 7(a), the classification performance of the model is quite high for the six sectoral classes (S1-S6). It can be seen that the model is able to correctly distinguish the sectoral samples and there is minimal confusion between the classes. The most successful classes are S1, S3 and S6 with accuracy and recall values of over 99%. Figure 7(b) shows the confusion matrix for the three regional classes (R2-R4). While the accuracy is high in this classification task, more confusion is observed between the classes. In particular, it is noticeable that classes R2 and R4 are confused with each other.

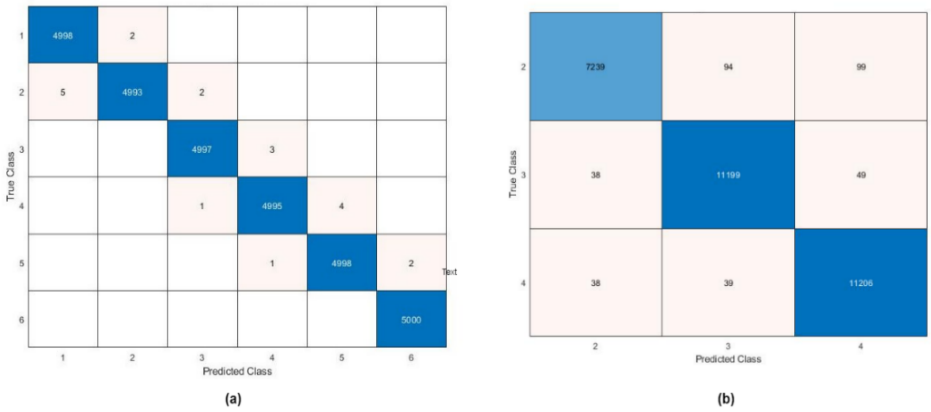

Figure 7. Confusion matrices of Wide neural network model. (a) for sector (b) for region.

It goes without saying that all artificial neural network methods have a high success rate in recognizing sectors. In region detection, Wide NN is the most successful method in terms of performance metrics. For this reason, the Wide NN method is favored in this study and proposed for both sector and region detection.

By integrating the Wide NN model into the inverter model created in the Matlab Simulink environment, phase voltages, phase currents, line to line voltages, sector and region values at the inverter output were analyzed. In the analysis carried out using the Wide NN model in the Simulink environment, the output parameters of the inverter were analyzed in detail. In this context, the phase voltage (Va), line to line voltage (Vab), the phase currents (Ia, Ib, Ic), the sector and region curves of the space vector and the results obtained are shown in Figures 8 and 9. These analyses were performed to evaluate the effectiveness of the Wide-NN model in detecting sectors and regions in inverters and to verify the performance of the system.

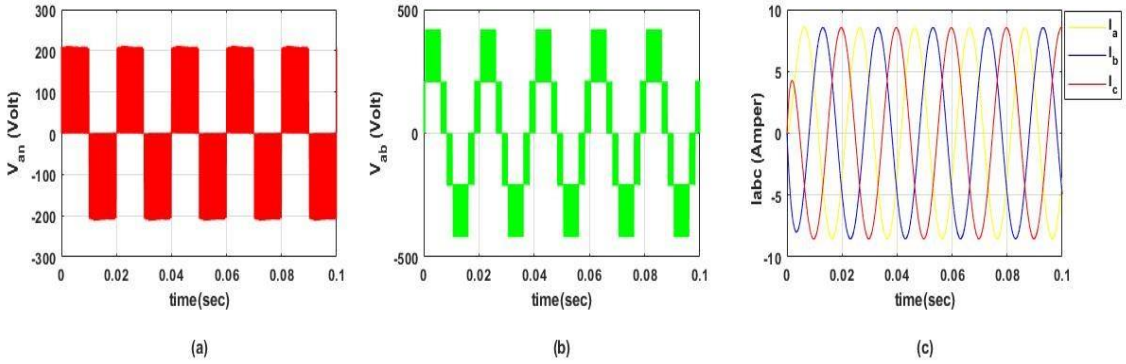

Figure 8. Inverter output simulation of Wide NN results (a) phase voltage (Va), (b) line-to-line voltage (Vab), (c) phase currents (Ia, Ib, Ic).

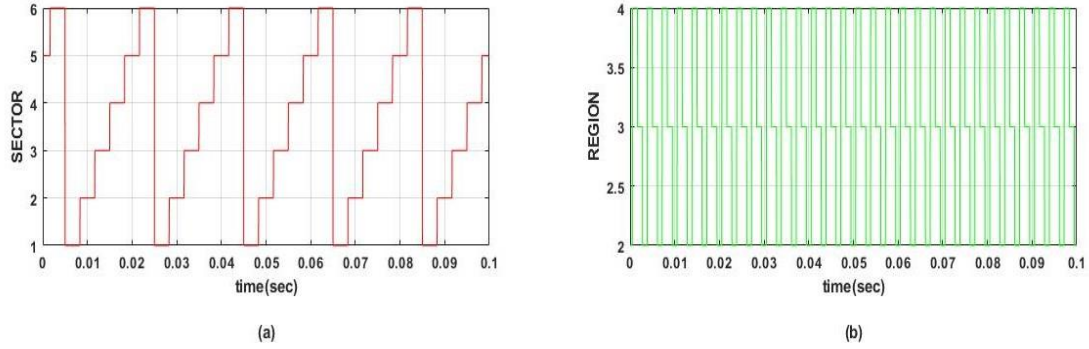

Figure 9. Inverter output space vector diagram simulation of Wide NN results (a) sector, (b) region.

The results of the Wide NN Matlab Simulink model show that the phase voltage fluctuates between 210.198 V and +210.198 V (Figure 8a). The simulation results for the line-to-line voltage (Vab) show that it fluctuates between +419.858 V and -419.858 V, as shown in Figure 8b. The phase currents at the output of the inverter are also shown in Figure 8c. The phase currents (Ia, Ib, Ic) have a peak-to-peak amplitude (p-p) of 16.890 A and a phase difference of 120° between them. Figure 9 shows the results of the space vector diagram at the inverter output. In the space vector analysis, it can be seen that the sector values vary between 1 and 6, while the region values are between 2 and 4.

C. Comparison of traditional and artificial neural network approaches

In this paper, a neural network-based approach for modelling a three-level inverter and detecting sectors and region is proposed. The effectiveness of the proposed approach is evaluated and compared with conventional simulation results. Table 7 summarizes the conventional simulation results and the performance results of the proposed neural network model.

Table 7. Performance comparison of the proposed approach.

Method	I (A)p-p	V_a (V)p-p	V_{ab} (V)p-p	Sector	Region
Simulation	17,102 A	396 V	796 V	1-6	2-4
Simulation with NN	16,890 A	420, 396V	839,716 V	1-6	2-4

In the results shown in Table 7, the output values obtained with the conventional simulation method reflect the theoretically optimal performance of the inverter. The simulation results with the Wide NN model show similar but slightly lower current values than the conventional simulation. The fact that the values for the sector and the region are the same shows the success of the neural network model.

In general, the results show that the proposed neural network model is suitable for the detection of sectors and region in inverters, but the accuracy may differ compared to conventional simulation methods. Although the neural network methods provide a simple and low-computation alternative for sector and region detection, they may require additional optimization due to certain deviations in the voltage-current outputs. Future studies can be conducted using machine learning and deep learning-based approaches to optimize inverter performance by investigating the detection of sectors and regions at different load values.

IV. CONCLUSION

In this paper, an artificial neural network-based approach for sector and region detection is proposed by modelling a three-level NPC type inverter. The Narrow, Medium, Wide, Bilayered and Trilayered based on ANNs were used to analyze and evaluate sectors and regions in the inverter. The classification performance of NN models is evaluated using performance metrics. The effectiveness of the proposed approach is tested using simulation results and its performance is evaluated. In this context, the most appropriate method for sector and region detection has been identified by applying ANN methods to the dataset obtained for a three-level NPC inverter. The study shows that the Wide NN method provides the best performance in sector and region detection. The results show that the Wide NN method can be a viable alternative for sector and region detection in inverters. The proposed Wide NN method can reduce the computational cost and optimize the process of sector and region detection, which is crucial for increasing the efficiency of inverters.

DECLARATIONS

Acknowledgements: The author/authors do not wish to acknowledge any individual or institution.

Author Contributions: Conceptualization, F.Ö., R.O.K. and T.V.M; methodology, F.Ö., R.O.K. and T.V.M.; software, F.Ö.; validation, F.Ö.; formal analysis, F.Ö., R.O.K. and T.V.M; resources, F.Ö., R.O.K. and T.V.M; data curation, F.Ö.; writing—original draft preparation, F.Ö., R.O.K. and T.V.M.; writing—review and editing, F.Ö., R.O.K. and T.V.M.; visualization, F.Ö.; supervision, R.O.K. and T.V.M.; project administration, R.O.K.;. All authors have read and agreed to the published version of the manuscript.

Conflict of Interest: The authors declare no conflicts of interest.

Supporting Institutions: This research received no external funding.

Ethical Approval: This study does not involve human or animal participants. All procedures followed scientific and ethical principles, and all referenced studies are appropriately cited.

Plagiarism Statement: This article has been evaluated for plagiarism, and no instances of plagiarism were detected.

Data Availability: The original contributions presented in this study are included in the article. Further inquiries can be directed at the corresponding author.

Use of AI Tools: The author/authors declare that no Artificial Intelligence (AI) tools were used in the creation of this article."

REFERENCES

Alharbi, M., & Altarjami, I. (2024). Dispatch optimization scheme for high renewable energy penetration using an artificial intelligence model. *Energies, 17*(12), Article 2799. https://doi.org/10.3390/en17122799

Annoukoubi, M., Essadki, A., & Akarne, Y. (2024). Model predictive control of multilevel inverter used in a wind energy conversion system application. *E-Prime – Advances in Electrical Engineering, Electronics and Energy, 9*, Article 100717. https://doi.org/10.1016/j.prime.2024.100717

Arslan, Ö. (2024). A machine learning approach for voice pathology detection using mode decomposition-based acoustic cepstral features. *Mathematical Modelling and Numerical Simulation with Applications, 4*(4), 469–494. https://doi.org/10.53391/mmnsa.1473574

Bakeer, A., Mohamed, I. S., Malidarreh, P. B., Hattabi, I., & Liu, L. (2022). An artificial neural network-based model predictive control for three-phase flying capacitor multilevel inverter. *IEEE Access, 10*, 70305–70316. https://doi.org/10.1109/ACCESS.2022.3187996

Cavdar, M., & Ozcira Ozkilic, S. (2024). A novel linear-based closed-loop control and analysis of solid-state transformer. *Electronics, 13*(16), Article 3253. https://doi.org/10.3390/electronics13163253

Chouhan, J., Gawhade, P., Ojha, A., & Swarnkar, P. (2024). A comprehensive review of hybrid energy systems utilizing multilevel inverters with minimal switch count. *Electrical Engineering, 107*, 8937-8961. https://doi.org/10.1007/s00202-024-02598-z

Cooper, M. I. (2022). Is mass related to latitude, longitude, and weather in Centrobolus Cook, 1897? *International Journal of Engineering Science Invention Research & Development, 9*(1), 27–32.

Dhiman, P., Kaur, A., Balasaraswathi, V. R., Gulzar, Y., Alwan, A. A., & Hamid, Y. (2023). Image acquisition, preprocessing and classification of citrus fruit diseases: A systematic literature review. *Sustainability, 15*(12), Article 9643. https://doi.org/10.3390/su15129643

Ghadi, Y. Y., Iqbal, M. S., Adnan, M., Amjad, K., Ahmad, I., & Farooq, U. (2023). An improved artificial neural network-based approach for total harmonic distortion reduction in cascaded H-bridge multilevel inverters. *IEEE Access, 11*, 127348–127363. https://doi.org/10.1109/ACCESS.2023.3332245

Hassan, Q., Algburi, S., Sameen, A. Z., Al-Musawi, T. J., Al-Jiboory, A. K., Salman, H. M., Ali, B. M., & Jaszczur, M. (2024). A comprehensive review of international renewable energy growth. *Energy and Built Environment*. https://doi.org/10.1016/j.enbenv.2023.12.002

Horiuchi, Y., Aoyama, K., Tokai, Y., Hirasawa, T., Yoshimizu, S., Ishiyama, A., Yoshio, T., Tsuchida, T., Fujisaki, J., & Tada, T. (2020). Convolutional neural network for differentiating gastric cancer from gastritis using magnified endoscopy with narrow band imaging. *Digestive Diseases and Sciences, 65*, 1355–1363. https://doi.org/10.1007/s10620-019-05898-9

Hossain, S., Biswas, S. P., Mondal, S., Islam, M. R., & Fekih, A. (2024). A capacitor voltage balancing hybrid PWM technique to improve the performance of T-type NPC inverters. *IEEE Access, 12*, 87545–87559. https://doi.org/10.1109/ACCESS.2024.3416834

Jayakumar, V., Chokkalingam, B., & Munda, J. L. (2021). A comprehensive review on space vector modulation techniques for neutral point clamped multilevel inverters. *IEEE Access, 9*, 112104–112144. https://doi.org/10.1109/ACCESS.2021.3100346

Kadhim, I. J., & Hasan, M. J. (2024). Enhancing power stability and efficiency with multilevel inverter technology based on renewable energy sources. *Electric Power Systems Research, 231*, Article 110290. https://doi.org/10.1016/j.epsr.2024.110290

Kapustin, A. V., & Shchurov, N. I. (2023). An overview of main multilevel inverter topologies. *Russian Electrical Engineering, 94*(5), 334–339. https://doi.org/10.3103/S1068371223050061

Khalid, M. (2024). Smart grids and renewable energy systems: Perspectives and grid integration challenges. *Energy Strategy Reviews, 51*, Article 101299. https://doi.org/10.1016/j.esr.2024.101299

Khan, M. U., Samer, S., Alshehri, M. D., Baloch, N. K., Khan, H., Hussain, F., Kim, S. W., & Zikria, Y. B. (2022). Artificial neural network-based cardiovascular disease prediction using spectral features. *Computers & Electrical Engineering, 101*, Article 108094. https://doi.org/10.1016/j.compeleceng.2022.108094

Kocalmış Bilhan, A., & Emikönel, S. (2022). Design of P&O and FL based MPPT controllers of PV array by using positive super lift DC/DC boost converter. *International Journal of Energy and Smart Grid, 7*(1–2), 36–46. https://doi.org/10.55088/ijesg.1201016

Krithiga, G., & Mohan, V. (2022). Elimination of harmonics in multilevel inverter using multi-group marine predator algorithm-based enhanced RNN. *International Transactions on Electrical Energy Systems, 2022*(1), Article 8004425. https://doi.org/10.1155/2022/8004425

Laib, A., Krim, F., Talbi, B., & Sahli, A. (2020). A predictive control scheme for large-scale grid-connected PV system using high-level NPC inverter. *Arabian Journal for Science and Engineering, 45*, 1685–1701. https://doi.org/10.1007/s13369-019-04182-1

Munawar, S., Iqbal, M. S., Adnan, M., Akbar, M. A., & Bermak, A. (2024). Multilevel inverters design, topologies, and applications: Research issues, current, and future directions. *IEEE Access, 12,* 149320 - 149350. https://doi.org/10.1109/ACCESS.2024.3472752

Pal, P. K., Jana, K. C., Siwakoti, Y. P., Majumdar, S., & Blaabjerg, F. (2022). An active-neutral-point-clamped switched-capacitor multilevel inverter with quasi-resonant capacitor charging. *IEEE Transactions on Power Electronics, 37*(12), 14888–14901. https://doi.org/10.1109/TPEL.2022.3187736

Qashqai, P., Babaie, M., Zgheib, R., & Al-Haddad, K. (2023). A model-free switching and control method for three-level neutral point clamped converter using deep reinforcement learning. *IEEE Access, 11*, 105394–105409. https://doi.org/10.1109/ACCESS.2023.3318264

Ramadan, E. A., Moawad, N. M., Abouzalm, B. A., Sakr, A. A., Abouzaid, W. F., & El-Banby, G. M. (2024). An innovative transformer neural network for fault detection and classification for photovoltaic modules. *Energy Conversion and Management, 314*, Article 118718. https://doi.org/10.1016/j.enconman.2024.118718

Sarhan, M. A., Barczentewicz, S., & Lerch, T. (2024). Hybrid islanding detection method using PMU-ANN approach for inverter-based distributed generation systems. *IET Renewable Power Generation, 18*(S1), 4453–4464. https://doi.org/10.1049/rpg2.13123

Sathik, M. J. (2023). A nine-level ANPC boosts type inverter topology with reduced component stress. *IEEE Transactions on Circuits and Systems II: Express Briefs, 71*(1), 380–384. https://doi.org/10.1109/TCSII.2023.3305230

Shiny, G., & Baiju, M. R. (2009). Space vector PWM scheme without sector identification for an open-end winding induction motor based 3-level inverter. In *Proceedings of the 35th Annual Conference of IEEE Industrial Electronics* (pp. 1310–1315). https://doi.org/10.1109/IECON.2009.5414649

Sirohi, V., Saggu, T. S., Kumar, J., & Gill, B. (2024). Implementation of a novel multilevel inverter topology with minimal components: An experimental study. *IEEE Canadian Journal of Electrical and Computer Engineering, 47*(1), 7–14. https://doi.org/10.1109/ICJECE.2023.3340326

Song, Z., Yang, S., & Zhang, R. (2021). *Does preprocessing help training over-parameterized neural networks?* Advances in Neural Information Processing Systems, 34, 22890–22904. https://arxiv.org/abs/2110.04622

Subbulakshmy, R., & Palanisamy, R. (2023). SVPWM control strategy for novel interleaved high gain DC converter fed 3-level NPC inverter for renewable energy applications. *ISA Transactions, 140*, 426–437. https://doi.org/10.1016/j.isatra.2023.05.019

Viswa Teja, A., Razia Sultana, W., & Salkuti, S. R. (2023). Performance explorations of a PMS motor drive using an ANN-based MPPT controller for solar-battery powered electric vehicles. *Designs, 7*(3), Article 79. https://doi.org/10.3390/designs7030079

Wang, Z., Liu, K., Ye, C., & Wan, S. (2025). Synchronized SVPWM schemes for closed-loop current control of three-level NPC inverters. *Journal of Power Electronics, 25*(12), 1490-1502. https://doi.org/10.1007/s43236-025-00999-2

Xue, C., Zhou, D., & Li, Y. (2020). Finite-control-set model predictive control for three-level NPC inverter-fed PMSM drives with LC filter. *IEEE Transactions on Industrial Electronics, 68*(12), 11980–11991. https://doi.org/10.1109/TIE.2020.3042156

Yan, H., Yang, J., & Zeng, F. (2022). Three-phase current reconstruction for PMSM drive with modified twelve-sector space vector pulse width modulation. *IEEE Transactions on Power Electronics, 37*(12), 15209–15220. https://doi.org/10.1109/TPEL.2022.3188425

Yan, Y., Wu, J., Cao, Y., Liu, B., Li, C., & Shi, T. (2024). An open-circuit fault diagnosis method for three-level neutral point clamped inverters based on multi-scale shuffled convolutional neural network. *Sensors, 24*(6), Article 1745. https://doi.org/10.3390/s24061745

Yarikkaya, S., & Vardar, K. (2023). Neural network-based predictive current controllers for three-phase inverter. *IEEE Access, 11*, 27155–27167. https://doi.org/10.1109/ACCESS.2023.3258679

Zhang, G., Band, S. S., Ardabili, S., Chau, K.-W., & Mosavi, A. (2022). Integration of neural network and fuzzy logic decision making compared with bilayered neural network in the simulation of daily dew point temperature. *Engineering Applications of Computational Fluid Mechanics, 16*(1), 713–723. https://doi.org/10.1080/19942060.2022.2043187

Zhang, S., Wang, R., Si, Y., & Wang, L. (2021). An improved convolutional neural network for three-phase inverter fault diagnosis. *IEEE Transactions on Instrumentation and Measurement, 71*, Article 3510915. https://doi.org/10.1109/TIM.2021.3129198